LA-UR-97-3483

Title: Status Report on a dc 130-mA, 75-keV Proton Injector*

CONF-9709158--

*Work performed under the auspices of the U.S. Department of Energy

Author(s): J. Sherman, A. Arvin, L. Hansborough, D. Hodgkins, E. Meyer, J. D. Schneider, H.V. Smith, Jr.,M. Stettler, R. R. Stevens, Jr., M. Thuot, and T. Zaugg, Los Alamos National Laboratory
Robin Ferdinand, CEA-Saiclay

Submitted to: 7th International Conference of Ion Sources
Taormina, Italy
September 7-13, 1997

Los Alamos
NATIONAL LABORATORY

DISCLAIMER

Status Report on a dc 130-mA, 75-keV Proton Injector

Joseph Sherman, Andrew Arvin, Lash Hansborough, David Hodgkins, Earl Meyer, J. David Schneider, H. Vernon Smith, Jr., Matthew Stettler, Ralph R. Stevens, Jr., Michael Thuot, and Thomas Zaugg

Los Alamos National Laboratory, Los Alamos, NM87545

Robin Ferdinand

CEA-Saclay, LNS, 91191 Gif-sur-Yvette Cedex, France

A 110-mA, 75-keV dc proton injector is being developed at Los Alamos. We use a microwave proton source coupled to a two solenoid, space-charge neutralized, low-energy beam transport (LEBT) system. The ion source produces 110-mA proton current at 75 keV using 600 - 800 W of 2.45 GHz input discharge power. Typical proton fraction is 85-90% of the total extracted ion current, and the rms normalized beam emittance after transport through a prototype 2.1 m LEBT is 0.20 (πmm-mrad). Beam space-charge neutralization is measured to be > 98% which enables the solenoid magnetic transport to successfully match the injector beam into a radio-frequency quadrupole (RFQ). Beam simulations indicate small emittance growth in the proposed 2.8 m low-energy demonstration accelerator (LEDA) LEBT. The LEBT also contains beam diagnostics, steering, and a beam deflector for variable duty factor and accelerator fast protect functions. The injector computer controls and reliability status are also discussed.

I. Introduction

In September, 1995 a report[1] was made on a proton source tech-base program leading towards the development of a dc 110-mA, 75-keV injector for 100-mA CW linacs.[2] The new injector is based on a microwave proton source[3] which operates at 2.45 GHz with a 875 G axial magnetic field. The ion source is coupled with a two-solenoid, LEBT system for matching into a RFQ.[4] In 1995, a specification list for the 75-keV injector was published, just as the first beam measurements were being made on a prototype of the low-energy demonstration accelerator[5] (LEDA) injector. The 1995 specification list with the 1997 status is

Table 1. 75-keV injector specifications and status.

Parameter	1995 Specification	1997 Status
Proton Beam Current (mA)	110	117
Proton Fraction (%)	85	90
Beam Energy (keV)	75	75
Discharge Power (W), Frequency (GHz)	300 - 450, 2.45	600 - 800, 2.45
Axial Magnetic Field (G)	920	875 - 960
Duty Factor (%)	100, (dc)	100, (dc)
Gas Flow (sccm)	2.8 - 8.5	2 - 5
Emission Aperture Radius (mm)	4.2	4.3
Extraction Gap (mm)	14.5	13.2
Beam Noise (%)	±1	±1
Ion Source Emittance (πmm-mrad)	0.13 (rms, normalized)	Not measured
RFQ Match point Emittance (πmm-mrad)	0.20 (rms, normalized)	0.20 (rms, normalized)
α_{RFQ}	1.944	1.944
β_{RFQ} (mm/mrad)	0.1193	0.1193

shown in Table 1. The 1995 goals have been achieved, and the injector work since 1995 leading to the 1997 status will be given here. The remaining item to be demonstrated is a flexible LEBT system for RFQ beam injection.

Section II addresses the 75-keV microwave proton-source design and performance. Beam current, proton fraction, beam emittance, and beam noise measurements were made on a prototype injector that has a magnetic solenoid LEBT section. These measurements indicate that a solenoid-magnet, beam space-charge (sc) neutralized LEBT is a good choice for matching the beam into a RFQ. Section III summarizes measurements and calculations relating the proton beam transport to an RFQ. These topics include proton beam sc neutralization measurements, first order design of the magnetic LEBT which includes beam focusing and steering, and higher-order beam transport calculations which predict some beam emittance growth from residual beam sc and solenoid lens aberration. Section III concludes with discussion of a LEBT design for flexible beam matching and control for injection into a RFQ. Section IV addresses injector computer control and beam availability tests.

II. 75 keV Ion Source

1. Ion source design, prototype injector, and beam diagnostics.

The proton source chosen for the LEDA project was originally developed at Chalk River Laboratories (CRL)[3,6]. Los Alamos modifications to the CRL ion source are summarized in a recent report.[7] The CRL plasma generator has been integrated to a 75-kV accel structure at Los Alamos (cf. Fig. 1). Plasma is generated by the interaction of 2.45 GHz microwaves with H_2 gas in the presence of an approximate 875 G axial magnetic field. The plasma is self-starting when the forward power P_f is greater than 300 W in the presence of the magnetic field and operating gas pressure. The 2.45 GHz magnetron discharge power supply is isolated from the 75-kV ion source potential by the rf high-voltage (HV) wave-guide break. The proton source solenoids are isolated from the 75-kV potential by a large polypropylene insulator. The source gas pressure is 1 - 2.5 mTorr , derived from the measured gas flow and the molecular flow conductance for the emission aperture radius R_{em} of 0.43 cm. The gas flow is controlled from ground level, which allows source operation without the complication of isolated power supplies. The ion-source HV is graded to ground over two 6.67 cm long alumina insulators by use of a 15 MΩ water resistor which gives 5 mA drain current. The insulators have an inside diameter of 40.6 cm.

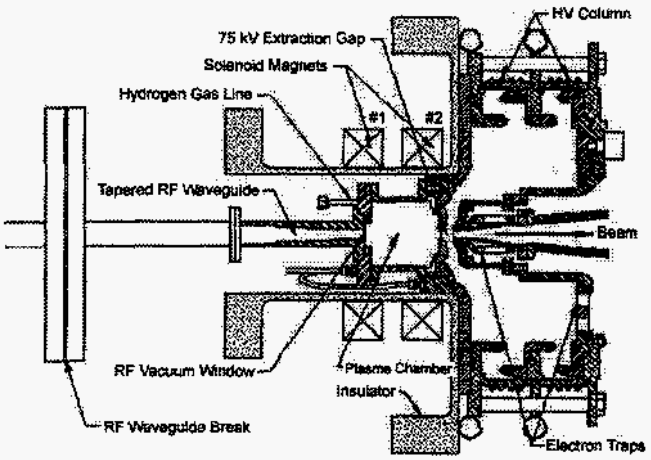

Figure 1. Line drawing of the 75-keV microwave proton source.

The 75-kV extraction voltage is held across a single 13.2 mm extraction gap g. After the plasma and first ground electrodes, there is an electron suppression electrode which prevents LEBT low-energy electrons from reaching the proton source. The final electrode of this tetrode accelerating structure is a second ground electrode which quickly establishes beam neutralization in the LEBT. A PBGUNS model[8] for this extraction system is shown in Fig. 2 for a 75-keV, 129-mA hydrogen ion beam. The effective mass of 2076 electron masses used in the Fig. 2 calculation is equivalent to 85% proton and 15% H_2^+ fraction. The design and testing of the HV column to reach 98% ion source availability is discussed in another paper at this conference.[9]

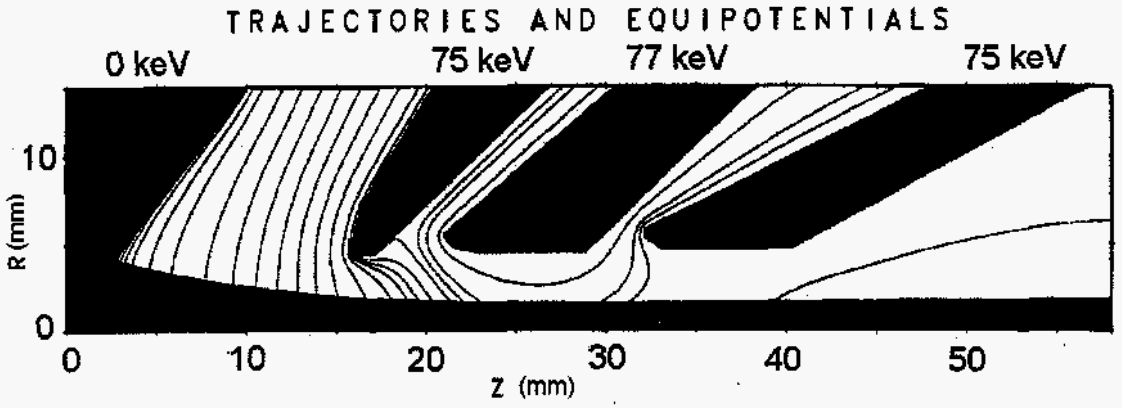

Figure 2. PBGUNS model for the tetrode extraction system used in the microwave proton source. The labeling at the top of the figure refers to the nominal beam energy at each electrode.

Beam measurements described in the following sections were made on a prototype injector shown in Fig. 3. The proton source (Fig. 1) is mounted on a beam diagnostics box which is followed by two solenoids. The beam is characterized by dc current monitors[10] (DC1 and DC2), an ac beam current transformer for beam noise measurements, an x and y video profile system for beam position and width measurements, and an emittance measuring unit (EMU), which also serves as a beam dump. Beam fraction measurements were made with a small dipole magnet located after the main EMU slit. Beam neutralization measurements were made with a four-grid energy analyzer located in the beam diagnostics box. The ion source gas load is pumped by a 2800 l/s turbopump H_2 on the diagnostics box and a 2500 l/s cryopump (H_2) on the EMU. The injector components and function are listed in Table 2 with their axial z position.

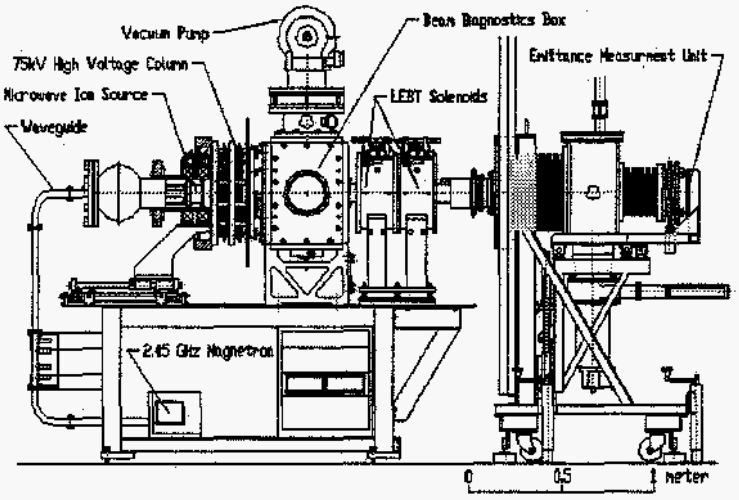

Figure 3. Prototype injector used for the beam measurements described in this report.

Table 2. Injector components and their axial location, z.

Injector Component	Function	z distance (cm)
Ion source extractor electrode	Beam formation	0.0
DC1	dc current measurement from the proton source	24.4
Video diagnostic (x,y)	Beam profile and position	42.2
Four-grid energy analyzer	Beam neutralization	43.8
AC toroid	Beam noise	51.0
Solenoid magnet entrance	Beam focus	78.9
DC2	dc current measurement through LEBT solenoids	129.6
EMU main slit	Beam emittance	213
Beam fraction diagnostic	Proton fraction	213

2. Beam current and proton fraction.

Figure 4 shows a plot of the DC1 beam current, I_b, vs. the forward power P_f from the 2.45 GHz magnetron with 5 sccm H_2 gas flow. The upper points refer to the beam current measured at DC1, and over 120 mA current is obtained for P_f = 680 W. A 90% proton fraction is typical from this ion source, so the 680 W point corresponds to 110 mA proton current in dc mode. The measured high-voltage power supply (HVPS) current has the same slope as DC1, but its magnitude is increased by the HVPS drain current. The ion source gas efficiency (at I_b = 0.122 A) is $\eta = 6.95 I_b/Q_{H2}(\text{sccm}) = 17\%$. The solid points give the beam current densities j (see the right scale) derived from I_b and R_{em} = 0.43 cm. A linear least squares straight line fit is shown through j, and the slope is a measure of the power efficiency $\xi = 0.20$ (mA/cm^2/W).

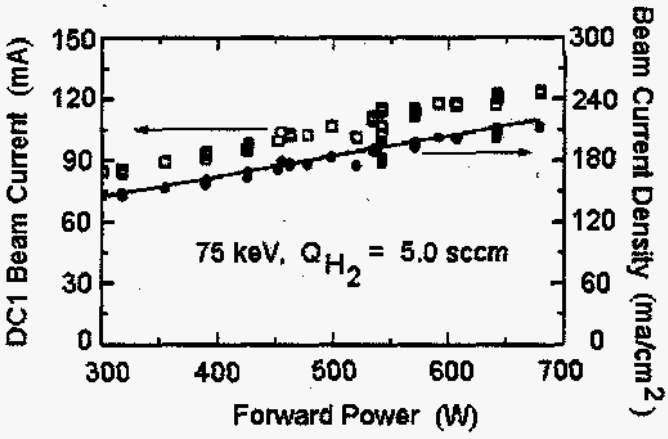

Figure 4. The dc proton beam current and beam current density measured vs. the 2.45 GHz magnetron forward power.

Beam current is sensitive to axial magnetic field tuning.[11] One of the best current-production modes is found with the proton-source solenoids separated by 12.1 cm and excited to 90 and 95 A. At the suggestion of the French Saclay group[12], this measured axial magnetic field was overlaid on the ion source profile. This is shown in Fig. 5 where the axial field measurements are plotted along the ion source body. The two vertical lines correspond to the position of the aluminum nitride microwave window and the ion source emission aperture. Within the accuracy of our measurements, both these lines intersect with the 875 G resonant magnetic field. Our conclusion is then the same as Saclay: one of the most efficient modes of source operation occurs with an ECR zone at both the entrance and exit of the source. The solid curve is an axial magnetic field prediction from the POISSON code.[13] This calculation includes the presence of ferromagnetic material introduced to increase the HV column reliability.[9] The calculation agrees with the measurements, especially at the positions of the 875 G fields.

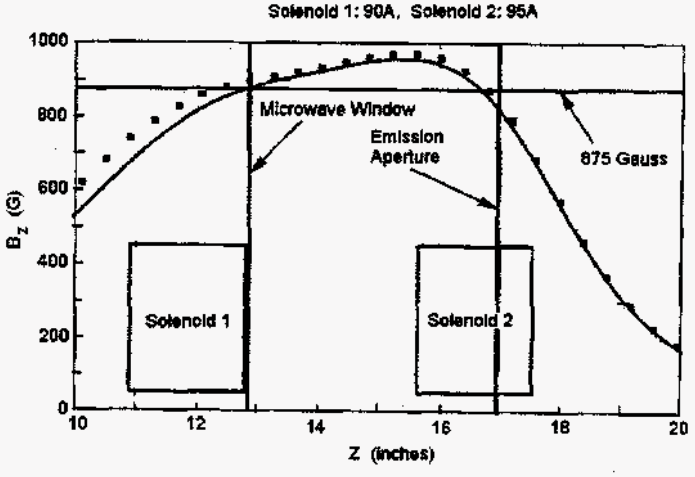

Figure 5. Measurement of the proton source axial magnetic field, and comparison of its magnitude at the entrance (microwave window) and exit (emission aperture) positions. Within errors, the resonant magnetic field of 875 G occurs at both locations.

The proton-beam fraction measurement is made by ramping the current in a small dipole magnet located immediately after the main EMU entrance slit. The EMU slit is 0.15 mm wide. The EMU Faraday cup, located 30 cm behind the main slit position, is then offset approximately 0.5 cm from the main slit. The magnetic field then sweeps the H^+, H_2^+, and H_3^+ species across the EMU Faraday cup slit. The mass resolution clearly separates the hydrogen-

ion species, as is shown in Fig. 6(A). This recent measurement was made at 50-keV beam energy while the injector was being tuned for an injector/RFQ test (see below). The LEBT solenoids (cf. Fig. 3) are off in order to prevent the spatial separation of the hydrogen-ion beam species. This technique shows the beam fraction at one location. The best measurement would be to analyze the whole beam for proton fraction.[14] In lieu of this measurement, Fig. 6(B) shows the proton fraction uniformity over the beam width made by repeated measurements with 1 cm EMU main slit displacements over the entire beam profile. These measurements show the proton fraction is 92-94%,

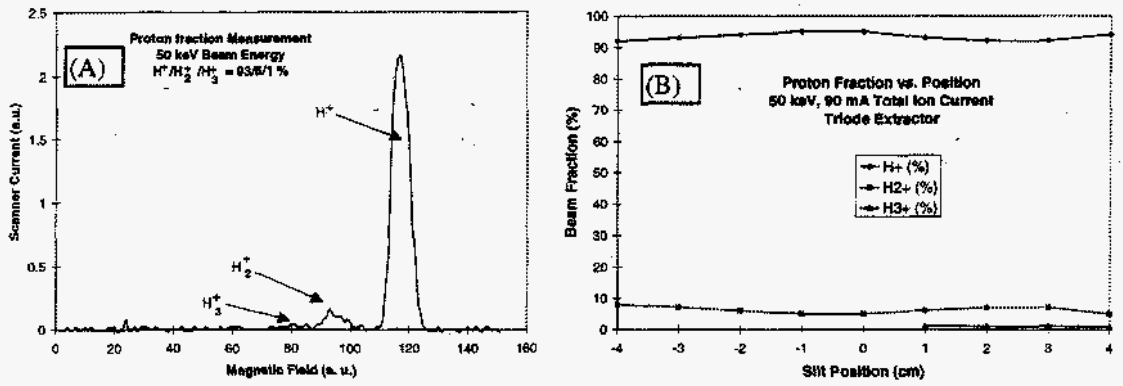

Fig. 6. (A) Proton beam fraction measurement near the beam center, and (B) proton fraction measurements made across the beam width in 1 cm step size. The lines in (B) are to guide the eye.

uniform across the beam.

Earlier work showed that by adding trace amounts of water to the plasma chamber, the proton fraction could be increased.[15] Measurements reported here were made without the addition of water. We have now found that operating the source with an oxygen plasma and beam for approximately 60 - 90 minutes before hydrogen operation effects a similar proton enhancement factor as the water catalysis. The proton fraction enhancement may be related to the removal of injector contaminants and/or plasma chamber wall modification leading to a wall chemistry more favorable to a high atomic hydrogen concentration,[16] and hence a higher-proton fraction source.[17]

3. Beam emittance and beam noise.

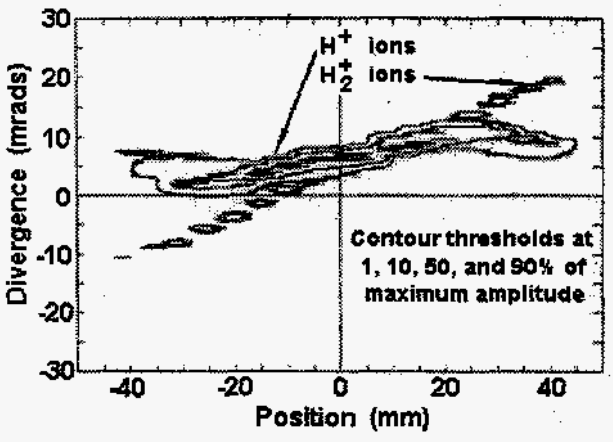

Figure 7. Measured phase-space distribution for a 130-mA, 75-keV hydrogen-ion beam.

A measured beam phase-space distribution is shown in Fig. 7 for a dc 130-mA, 75-keV beam. The proton fraction for this measurement is 90%, thus the proton current is 117 mA. The measurement was made with a two-slit device[18] (EMU) which includes a high-power beam dump. Contour thresholds are shown at 1, 10, 50, and 90% of the maximum current amplitude recorded in the EMU Faraday cup. The H_2^+ ions are seen at the lowest threshold. A Gaussian extrapolation procedure[19] is used to extract the rms normalized proton emittance of 0.20 (πmm-mrad) from the phase-space measurement shown in Fig. 7. The LEBT solenoids were set to 0.17 T to transport the beam to the EMU location. Some third-order aberration is evident at large radii in Fig. 7. This probably arises from a spherical aberration in the LEBT solenoid, whose inside diameter is 10 cm (see below).

The beam noise power spectrum as a function of frequency f_b has been measured with an AC toroid located at z = 51 cm (cf. Table 2). Two beam noise measurements are shown in Fig. 8(A) for 75-keV beam. The noise power spectra were obtained with a HP8561E spectrum analyzer. The curves in Fig. 8(A) were taken with a 30 kHz resolution bandwidth (1 MHz coherent oscillation, 130 mA), and the

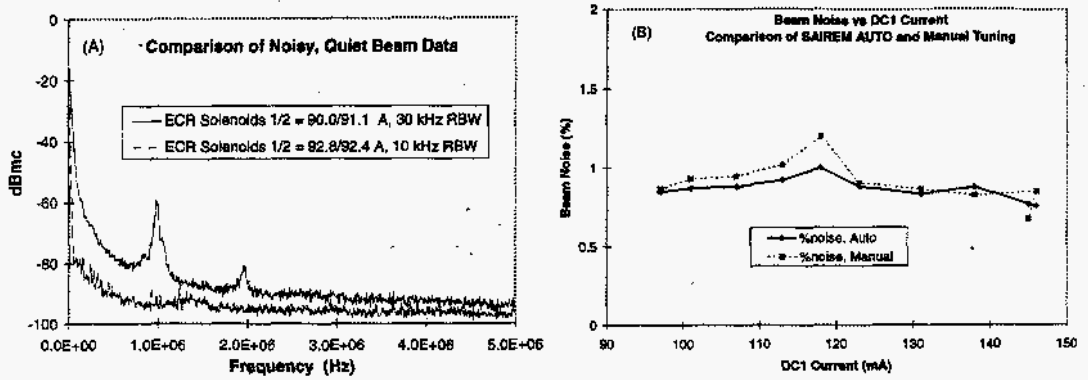

Figure 8. (A) Power spectrum measured for a 75 keV, 130 mA hydrogen-ion beam. For one case, the source magnetic field is tuned to give a coherent oscillation at 1 MHz, and in the second case, a change in magnetic field eliminates the coherent oscillation. (B) Summary of beam noise measurements made as a function of I_b. These measurements correspond to the "noisy" tune shown in (A).

second was taken with 10 kHz resolution bandwidth (105 mA) in a more quiescent mode where the coherent oscillations are eliminated. The 1 - 2 MHz oscillations may be related to the proton cyclotron frequency which is 1.33 MHz at 0.0875 T.

An rms beam noise is found by summing the power to f_b = 5 MHz (P_{sum}), and then deriving an rms voltage $v_{rms} = (P_{sum}*50)^{1/2}$ where the input impedance of the HP8561E is 50Ω. Using a test signal, the toroid has a measured uniform response to 10 MHz. The power sum is taken for f_b > 100 kHz because the beam sc neutralization is effective for canceling sc oscillations with f_b < 100 kHz (see below). The rms beam current noise $i_{rms} = v_{rms}$ T is then derived from the toroid transfer function T = (1A/V). A plot of the beam noise (%), which is $(i_{rms}/I_b)*100$, is then shown in Fig. 8(B). The I_b = 130 mA magnetic field settings are used in the Fig. 8(B) data. The two curves shown in Fig. 8(B) correspond to two separate tuning procedures. The first is acquiring the noise spectrum after a SAIREM four-stub tuner has automatically tuned the forward and reverse power (AUTO), while the second set shows results after the tuner was manually adjusted to reduce the reflected power. For most DC1 currents, the AUTO procedure gives a slightly lower beam noise.

III. Low Energy Beam Transport System

1. Beam sc neutralization measurement.

The degree of proton beam sc neutralization (f) is required for magnetic LEBT designs. An effective beam current may be defined as $I_{eff} = (1 - f)I_b$, and I_{eff} may then be used in beam transport codes such as TRACE[20] and SCHAR.[21] A non-interceptive gridded-energy analyzer has been used to measure f as a function of gas density in the LEBT and total hydrogen-ion beam current.[22] The method relies on measuring the potential within the beam volume by measuring the energy distribution of the slow ions ejected from the beam plasma. The width of the measured distribution is $\Delta\phi$, and the beam neutralization parameter f is derived from $f = 1 - \Delta\phi/\Delta\phi_u$ where $\Delta\phi_u = i_b R/\beta$ = voltage drop across an unneutralized, uniform beam with current I_b, velocity β, and $R = 30\Omega$. For 0.13 A, a 75 keV proton beam has $\Delta\phi_u$ = 308 V. The results for f in % are shown in Figs. 9(A) and 9(B). The beam energy is 75 keV. Figure 9(A)

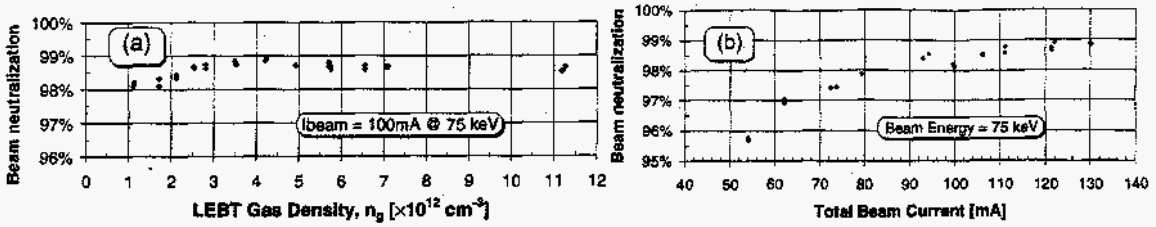

Figure 9. Plot of beam neutralization, f, vs. (a) the H_2 gas density in the LEBT, and (b) total beam current.

shows f as a function of the LEBT H_2 gas density n_g, and 9(B) shows f as a function of the beam current. For our typical operation of $n_g = 1 - 2 \times 10^{12}$ (cm)$^{-3}$ H_2 and $I_b > 100$ mA, f is in the 98 - 99% range.

The beam sc neutralization time constant may be derived from $\tau = (n_g \sigma_e v_b)^{-1} = 7$ μs, where v_b = beam velocity = βc and $\sigma_e = 2.5 \times 10^{-16}$ cm^2 is the total electron production cross section at 75 keV proton beam energy in H_2 gas. This suggests that beam ionization of the background gas is effective in neutralizing oscillating beam sc for $f_b < 100$ kHz. A review of intense ion-beam sc neutralization processes is found in ref. [23].

2. Magnetic solenoid beam transport.

The first choice for beam transport is use of a two-solenoid beam transport system[4], which takes advantage of background gas ionization to neutralize the beam sc. Although some proton beam emittance growth was observed in 50-keV single-solenoid LEBT[1] measurement, and in the present 75-keV, 130-mA measurement, the LEBT output beam emittances meet the LEDA project goals of 0.20(πmm-mrad), rms normalized (cf. Table 1). The 50-keV LEBT and the 75-keV measurements (cf. previous section) were made in 1.65 m and 2.1 m long LEBTs. The causes of beam emittance growth are thought to be third-order aberrations[24] in the LEBT solenoid lenses, and beam current fluctuations (noise) which can cause an effective emittance growth.[25] An example of beam emittance growth in the magnetic solenoid is shown in Fig. 10 where the 10% contour of Fig. 7 phase-space data is plotted with the higher-order SCHAR[21] code predictions.[11] The onset of the third-order aberration is observed and predicted by the SCHAR code. These data are from the 2.1 m LEBT shown in Fig. 3.

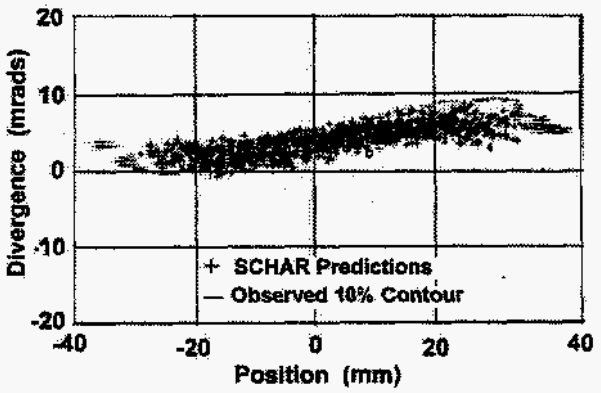

Figure 10. Comparison of the measured 10% threshold contour with a higher-order (SCHAR) beam transport calculation. The measurement is as in Fig. 7 where the beam current is 130-mA at 75-keV energy.

The LEDA baseline LEBT design is shown in Fig. 11. It is 2.8 m long, and its functions include beam focusing and steering at the RFQ match point, dc beam current and beam noise diagnosis, and beam location and beam FWHM measurements made with non-interceptive video diagnostics located at three stations along the beam line. Beam duty factor and accelerator run permit functions are controlled by the kicker magnet located in box 2. An insertable plunging beam stop is planned to stop the 130-mA, 75 keV beam. It will also serve as the beam stop when the kicker magnet is in operation. A beam kicker has proven reliable and effective in the Paul Scherrer LEBT system.[14] A variable beam iris will control the dc beam current level, and may be used to tune the following linac structures. A beam envelope angle of 55 mrad at the RFQ match point allows the insertion of a third pump/diagnostics box at the RFQ entrance.

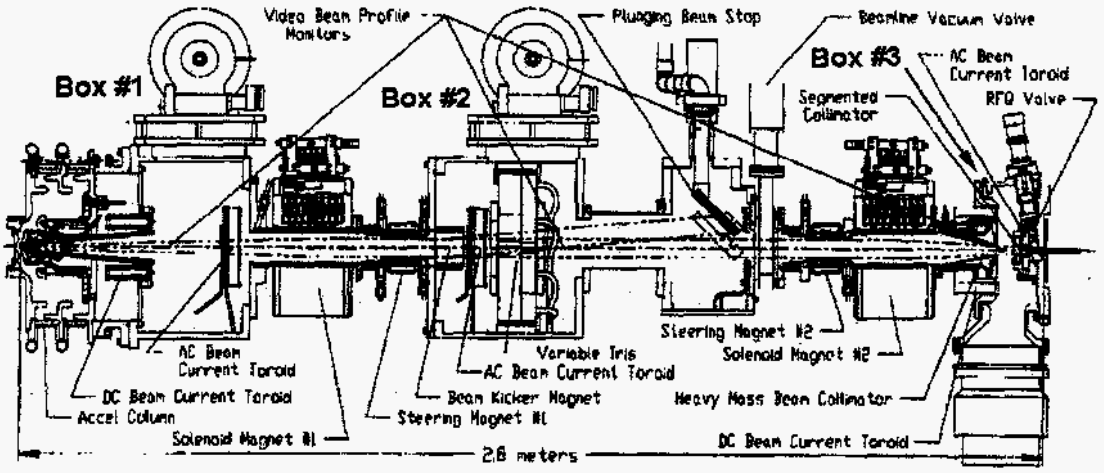

Figure 11. A proposed 2.8 m long LEBT for the LEDA project..

The codes TRACE[20] and SCHAR[21] have been used to model the LEDA injector beam at the RFQ matchpoint.[24] Phase-space measurements made with the prototype injector (Fig. 3) are drifted back to the ion source using the TRACE code, using the emission aperture radius to determine a range of f values. This procedure yields f = 0.97 - 0.995 in agreement with the beam sc neutralization measurements (cf. Section III.1). TRACE has been used to calculate the tuning curves shown in Fig. 12(A). Here the (α,β)

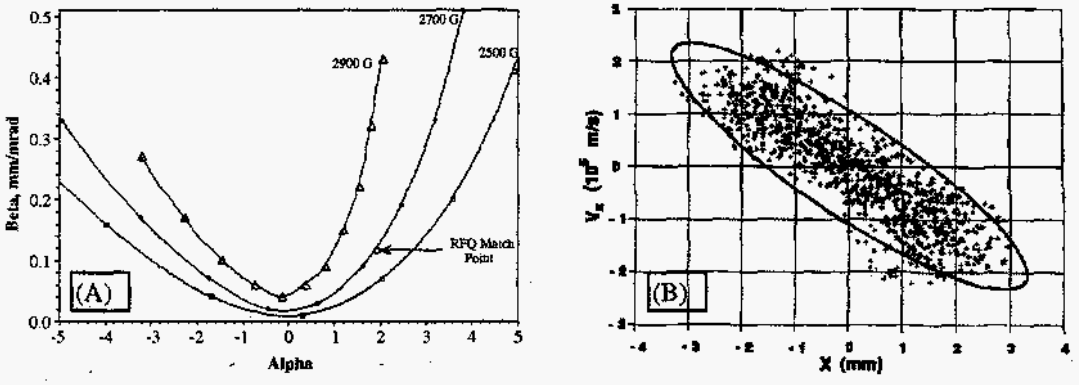

Fig. 12(A) shows the (α,β) tuning diagram for the 2.8 m LEBT shown in Fig. 11. The higher-order code SCHAR shows the predicted injector beam superimposed on the LEDA RFQ acceptance ellipse in Fig. 12(B).

Courant-Snyder parameters are plotted with a fixed B field in solenoid 1 and the solenoid 2 current is varied to trace a curve in (α,β) matching space. The LEDA RFQ matching parameters are α = 1.909 and β = 0.1175 mm/mrad. These conditions are achieved for $B_{sol\#1}$ = 2700 G and $B_{sol\#2}$ = 3667 G, and are easily within the capability of the LEBT solenoid magnets.

Figure 12(B) shows the SCHAR-calculated phase-space for the 2.8 m LEBT (Fig. 11). The superimposed ellipse is the RFQ acceptance for a 100-mA, 0.20 (πmm-mrad) emittance injector beam. SCHAR predicts the beam emittance is 0.23 (πmm-mrad) at the RFQ match point. The PARMTEQM RFQ code[24] then predicts that 93% of this beam (106 mA) will be transmitted through the RFQ with the output 6.7 MeV emittance being 0.21 (πmm-mrad).

III. Computer Control and Reliability Tests

The LEDA injector control system, based on the EPICS toolkit,[26] provides man/machine interface through a graphical user interface, automated machine sequencing, machine protection interlocks, run permit, and data archiving. Injector automation and reliability requirements are best addressed with a layered approach which distributes the interlock and run permit functions across the injector control subsystems. This procedure provides redundancy and automatic handling of subsystem configurations which aids in injector debugging by allowing some subsystem operation even though the injector may not be fully operational. This approach breaks the machine into functional layers, starting from basic personnel protection and progressing through machine protection, subsystem operation, subsystem automation, machine operation (involving multiple subsystems), and finally, machine automation. Each functional layer is dependent only on lower layers, and is independent of any higher layer's functionality. In this way, complex machine operation can be achieved incrementally without compromising basic system operation. In particular, failure of automation or sequencing logic cannot force the machine into an unsafe operating condition. An interesting side effect of this approach is that run permit and much of the interlock logic is tightly coupled to individual subsytems, making these functions difficult to distinguish from control logic. While this requires an intimate knowledge of the injector operation from control personnel, it allows a level of robust operation not achievable in the past.

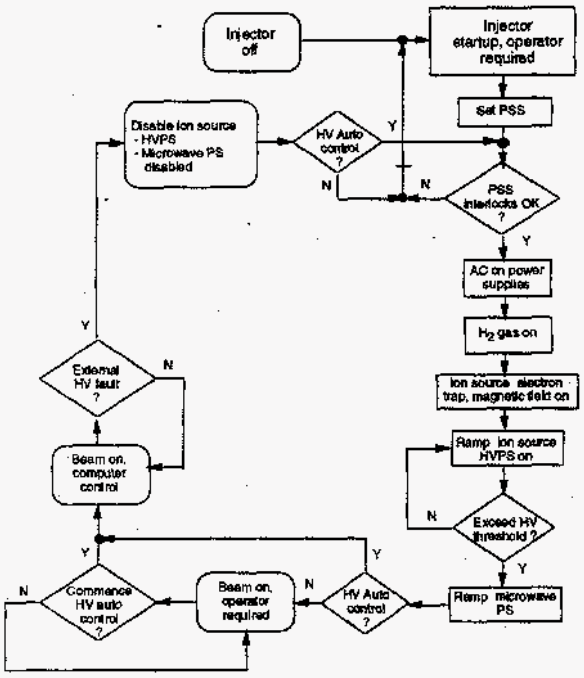

Figure 13. Sequencing used by the EPICS control system to operate the LEDA injector. The control system automatically recovers injector beam after a high-voltage spark event.

The primary automation functions provided by the control system involve semi-automatic start-up, automatic high voltage sparkdown recovery, and detection of abnormal operation. The control system enforces a particular sequence of operations to start the injector. Operators may set all parameters to operating conditions, and the subsystem interlock/run permit logic determines the time that the hardware is activated. This automation is a direct result of the functional architecture and required no additional effort to implement. Since the injector periodically experiences high voltage faults, the high voltage sparkdown recovery is the most visible automation function. The high voltage power supply is controlled by state machine[27] automation which is responsible for high voltage on/off and the sequencing necessary for overload recovery, as shown in Fig. 13. Also included is logic to limit the number of recovery attempts in the face of continuous faults, and to return to manual mode after an interlock fault. In order to reduce the vigilance required by operators during long term operation, logic has been implemented which (when armed by the operator) automatically detects normal operation, and commands the machine to a safe "off" state when an unexpected deviation occurs. Expected deviations, such as spark down detection and recovery, do not cause an injector shutdown.

The injector completed a week long run of 168 hours operation time. Of this time, the injector operated at 75 keV, > 120 mA for 161.3 hours (96% available). The ion source accounted for 3.4 hours of beam off time because of recovery from HV sparks. This corresponds to 98% ion source availability. The beam availability as a function of elapsed run is shown in Fig. 14. Achieving this performance required a comprehensive high-voltage column design, and is the subject of a companion paper[9] at this conference. The first version of the LEDA injector, without the beam kicker shown in Fig. 11, is now being attached to the CW 1.25 MeV CRITS RFQ[28]. The LEDA LEBT design concepts will be tested on the operational CRITS RFQ in the latter part of 1997 before operation of the 6.7 MeV LEDA RFQ in 1998.

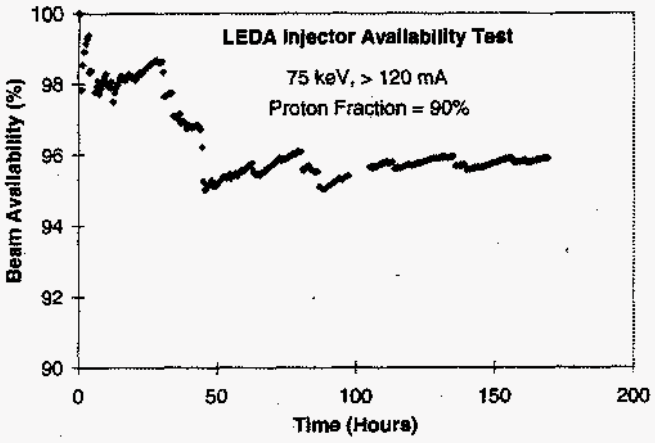

Figure 14. LEDA injector beam availability as a function of the elapsed run time.

Acknowledgments

We thank Chalk River Labs, especially Terry Taylor, John Wills, and Gerry McMichael for their technical support. Our collaboration with the injector group working on the French IPHI project (CEA-Saclay) is very helpful. We also thank the US Department of Energy for the financial support required to complete this work.

References:

[1]J. Sherman, G. Bolme, C. Geisik, D. Gilpatrick, L. Hansborough, D. Hodgkins, P. Lara, E. Meyer, J. Power, C. Rose, D. Sandoval, P. Schafstall, J. D. Schneider, M. Stettler, R. Stevens, Jr., M. Thuot, R. Wright, and T. Zaugg, Rev. Sci. Instrum. 67(3),1296(1996).

[2]G. Lawrence, et. al., in the Proceedings of the XVIII International Linear Accelerator Conference, CERN 96-07, (Geneva, Switzerland), (June, 1996), 710.

[3]Terence Taylor and Jozef F. Mouris, Nuclear Instrum. And Methods in Phys. ResearchA336, 1(1993).

[4]Ralph R. Stevens, Jr., AIP Conference Proceedings No. 287, 646(1992).

[5] J. D. Schneider and K. C. D. Chan, in the Proceedings of the 1997 Particle Accelerator Conference, (Vancouver, B.C.), (May, 1997), to be published.

[6]Terence Taylor and John S. C. Wills, Nuclear Instrum. And Methods in Phys. ResearchA309, 37(1991).

[7]L. D. Hansborough, D. J. Hodgkins, E. A. Meyer, J. David Schneider, J. D. Sherman, R. R. Stevens, Jr., and T. J. Zaugg, Proceedings of the 1997 Particle Accelerator Conference, Vancouver, BC, Canada (May 12-16, 1997), to be published.

[8]Jack E. Boers, Proceedings of the 1995 Particle Accelerator Conference, IEEE Catalog Number 95CH35843, Dallas, Texas (May 1-5, 1995), 2312.

[9]Joseph Sherman, Andrew Arvin, Lash Hansborough, Dave Hodgkins, Earl Meyer, J. David Schneider, R. R. Stevens, Jr., and Thomas Zaugg, these proceedings, and LA-UR-97-3282.

[10]K. B. Unser, Proc. Of the 1989 Particle Accelerator Conference (Chicago, Il), IEEE Catalog Number 89CH2669-0, 71 (1989).

[11]J. D. Sherman, G. O. Bolme, L. D. Hansborough, D. J. Hodgkins, M. E. Light, E. A. Meyer, J. D. Schneider, H. V. Smith, Jr., M. W. Stettler, R. R. Stevens,Jr., M. E. Thuot, and T. J. Zaugg, Proceedings of the XVIII International Linear Accelerator Conference, CERN 96-07, (Geneva, Switzerland), (June, 1996), 701.

[12]P-Y. Beauvais, P. Ausset, D. Bogard, O. Delferriere, J. Faure, R. Ferdinand, A. France, R. Gobin, P. Gros, J-M. Lagniel, and P-A. Leroy, Proceedings of the 1997 Particle Accelerator Conference, Vancouver, BC, Canada (May 12-16, 1997), to be published.
[13]James H. Billen and Lloyd M. Young, Proceedings of the 1993 Particle Accelerator Conference, IEEE Catalog Number 93CH3279-7, Washington, D.C. (May 17-20, 1993), 790.
[14]M. Olivo, E. Mariani, and Joseph Sherman, Rev. Sci. Instrum. 63(4), 2714(1992).
[15]D. Spence, G. McMichael, K. R. Lykke, J. D. Schneider, J. Sherman, R. Stevens, Jr., and D. Hodgkins, Rev. Sci. Instrum. 67 (4), 1642(1996).
[16]David Spence and Orville J. Steingraber, Rev. Sci. Instrum. 59(11), 2464(1989).
[17]Chun Fai Chan, C. F. Burrell, and William S. Cooper, J. Appl. Phys. 54(11), 6119(1983).
[18]T. Taylor, M. S. de Jong, and W. L. Michel, Proceedings of the 1988 Linear Accelerator Conf., CEBAF-Report-89-001, 100(1988).
[19]Paul Allison, Joseph D. Sherman, and H. Vernon Smith, Jr., "Comparison of Measured Emittance of an H^- Beam with a Simple Theory", Los Alamos Report LA-8808-MS (June, 1981).
[20]K. R. Crandall and D. P. Rusthoi, Los Alamos National Lab Report LA-UR-90-4146 (1990).
[21]Mark J. Jakobson and Richard J. Hayden, Nucl. Instrum. And Methods A **258**, 536 (1987).
[22]Robin Ferdinand, Joseph Sherman, Ralph R. Stevens, Jr., and Thomas Zaugg, Proceedings of the 1997 Particle Accelerator Conference, Vancouver, BC, Canada (May 12-16, 1997), to be published.
[23]I. A. Soloshenko, Rev. Sci. Instrum.67(4), 1646 (1996).
[24]H. Vernon Smith, Jr., Joseph D. Sherman, Ralph R. Stevens, Jr., and Lloyd M. Young, Proceedings of the 1997 Particle Accelerator Conference, Vancouver, BC, Canada (May 12-16, 1997), to be published.
[25]Paul Allison, IEEE Trans. Nucl. Sci. **NS-32**, 2556 (1985).
[26]Leo R. Dalesio, Jeffrey O. Hill, Martin Kraimer, Stephen Lewis, Douglas Murray, Stephan Hunt, William Watson, Matthias Clausen, and John Dalesio, Nucl. Instrum. And Methods in Phys. Res. A 352, 179(1994).
[27]Kevin Skahill, VHDL for Programmable Logic, Addison-Wesley Publishing Co., 231(1996).
[28]J. David Schneider, Jerry Bolme, Vaughn Brown, Martin Milder, George Neuschaefer, Daniel Rees, Patrick Schafstall, Joseph Sherman, Ralph R. Stevens, Jr., Thomas Zaugg, G. E. McMichael, Javid Sheikh, and Terence Taylor, Proceedings of the 1994 International Linac Conference, Tsukuba, Japan, 149 (May, 1994).